

Online Probabilistic Model Identification using Adaptive Recursive MCMC

Pedram Agand^{1*}, Mo Chen¹, and Hamid D. Taghirad²

¹Department of Computer Science, Simon Fraser University, Burnaby, BC, Canada.

²Department of Electrical Engineering, K. N. Toosi University of Technology, Tehran, Iran.

Abstract

The Bayesian paradigm provides a rigorous framework for estimating the whole probability distribution over unknown parameters, but due to high computational costs, its online application can be difficult. We propose the Adaptive Recursive Markov Chain Monte Carlo (ARMCMC) method, which calculates the complete probability density function of model parameters while alleviating the drawbacks of traditional online methods. These flaws include being limited to Gaussian noise, being solely applicable to linear in the parameters (LIP) systems, and having persisting excitation requirements (PE). A variable jump distribution based on a temporal forgetting factor (TFF) is proposed in ARMCMC. The TFF can be utilized in many dynamical systems as an effective way to adaptively present the forgetting factor instead of a constant hyperparameter. The particular jump distribution has tailored towards hybrid/multi-modal systems that enables inferences among modes by providing a trade-off between exploitation and exploration. These trade-off are adjusted based on parameter evolution rate. In comparison to traditional MCMC techniques, we show that ARMCMC requires fewer samples to obtain the same accuracy and reliability. We show our method on two challenging benchmarks: parameter estimation in a soft bending actuator and the Hunt-Crossley dynamic model. We also compare our method with recursive least squares and the particle filter, and show that our technique has significantly more accurate point estimates as well as a decrease in tracking error of the value of interest.

Introduction

Bayesian methods are powerful tools to not only obtain a numerical estimate of a parameter but also to give a measure of confidence (Bishop 2006; Joho et al. 2013). This is obtained by calculating the probability distribution of parameters rather than a point estimate, which is prevalent in frequentist paradigms (Tobar 2018). One of the main advantages of probabilistic frameworks is that they enable decision making under uncertainty. In addition, knowledge fusion is significantly facilitated in probabilistic frameworks; different sources of data or observations can be combined according to their level of certainty in a principled manner (Agand and Shoorehdeli 2019). Using credible intervals instead of confidence intervals (Kuśmierczyk, Sakaya, and

Klami 2019), an absence of over parameterized phenomena (Bishop 2006), and evaluation in the presence of limited number of observed data (Joho et al. 2013) are other distinct features of this framework.

Nonetheless, Bayesian inference requires high computational effort for obtaining the whole probability distribution and requires prior general knowledge about the noise distribution. Consequently, strong simplifying assumptions were often made (e.g. calculating specific features of the model parameters distribution rather than the whole distribution). One of the most effective methods for Bayesian inferences is Markov Chain Monte Carlo (MCMC). In the field of system identification, MCMC variants such as the one proposed by (Green 2015) are mostly focused on offline system identification. This is partly due to computational challenges which prevent its real-time use. There are extensive research in the literature which investigate how to increase sample efficiency (e.g. (Welling and Teh 2011; Nori et al. 2014; Mandel et al. 2016)). The authors in (Green 1995) first introduced reversible jump Markov chain Monte Carlo (RJMCMC) as a method to address the model selection problem. In this method, an extra pseudo-random variable is defined to address dimension mismatch. There are further extensions of MCMC in the literature; however, there is a lack of variants suitable for online estimation. One example which claims to have often much faster convergence is No-U-Turn Sampler (NUTS), which can adapt proposals “on the fly” (Hoffman, Gelman et al. 2014).

If the general form of the relation between inputs and outputs is known either by physical relation or knowing the basis function, parametric identification techniques are an effective way to model a system. To identify the parameters in a known model, researchers propose frequency ((Lin 2019)) or time domain ((Agand et al. 2022)) approaches. Noisy measurements, inaccuracy, inaccessibility, and costs are typical challenges that limit direct measurement of unknown parameters in a physical/practical system (Agand, Taghirad, and Khaki-Sedigh 2016). Parameter identification techniques have been extensively used in different subject areas including but not limited to chemistry, robotics, fractional models and health sectors (Yang et al. 2020; Kim et al. 2019; Yu et al. 2022; Houssein et al. 2021). For instance, motion filtering and force prediction in robotics applications are important fields of study with interesting chal-

*pagand@sfu.ca

lenges which makes them suitable test cases for Bayesian inferences (Saar, Giardina, and Iida 2018).

Different parametric identification methods have been proposed in the literature for linear and Gaussian noise (Wang, Sekhon, and Qi 2018); however, in cases of nonlinear hybrid/multi-modal systems (e.g. Hunt-Crossley or fluid soft bending actuator) or systems with non-Gaussian noise (e.g. impulsive disturbance), there is no optimal solution for the identification problem. In addition, in cases that the assumed model for the system is not completely valid, MCMC implementation of Bayesian approach can provide reasonable inferences. Authors in (Wang et al. 2019) utilize the least square methods for nonlinear physical modeling of air dynamics in pneumatic soft actuator. Carvalho and Martins (2019) proposed a method to determine the damping term in the Hunt-Crossley model. A single-stage method for the estimation of the Hunt-Crossley model is proposed by (Haddadi and Hashtrudi-Zaad 2012) which requires some restrictive conditions to calculate the parameters. Moreover, the method does not offer any solution for discontinuity in the dynamic model, which is common in the transition phase from contact to free motion and vice versa (Williams et al. 2018).

This paper proposes a new technique, Adaptive Recursive Markov Chain Monte Carlo (ARMCMC), to address several weaknesses of traditional online identification methods, such as solely being applicable to systems Linear in Parameters (LIP), having Persistent Excitation (PE) requirements, and assuming Gaussian noise. ARMCMC is an online method that takes advantage of the previous posterior distribution whenever there is no abrupt change in the parameter distribution. To achieve this, we define a new *variable jump distribution* that accounts for the degree of model mismatch using a *temporal forgetting factor*. The temporal forgetting factor is computed from a model mismatch index and determines whether ARMCMC employs modification or reinforcement to either restart or refine the estimated parameter distribution. As this factor is a function of the observed data rather than a simple user-defined constant, it can effectively adapt to the underlying dynamics of the system. We demonstrate our method using two different examples: a soft bending actuator and the Hunt-Crossley model. We show favorable performance compared to the state-of-the-art baselines.

Preliminaries

Problem statement

In the Bayesian paradigm, parameter estimations are given in the form of the posterior probability density function (pdf); this pdf can be continuously updated as new data points are received. Consider the following general model:

$$Y = F_j(X, \theta_j) + \nu_j, \quad \forall j \in \{1, 2, \dots, m\}, \quad (1)$$

where Y , X , θ , and ν are concurrent output, input, model parameters set and noise vectors, respectively. For a hybrid system, there can be m different nonlinear functions (F_j) with different parameters set (θ_j) for each mode. For multi-modal systems, there can be m different noise distribution ν_j

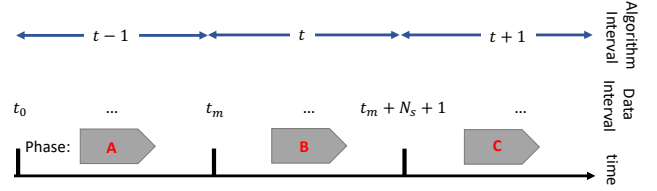


Figure 1: Data timeline and different phases of ARMCMC algorithm. For algorithm at time t : Phase (A) Data collection [N_s data points are packed for the next algorithm time step], Phase (B) Adjustment [the method is applying to the most recent pack], (C) Execution [after the min evaluation of algorithm, the results will be updated on posterior distribution and any byproduct value of interest].

for each mode. To calculate the posterior pdf, the observed data (input/output pairs) along with a prior distribution are combined via Bayes' rule (Khatibisepehr, Huang, and Khare 2013). For more information please refer to the supplementary material. We will be applying updates to the posterior pdf using batches of data points; hence, it will be convenient to partition the data as follows:

$$D^t = \{(X, Y)_{t_m+1}, (X, Y)_{t_m+2}, \dots, (X, Y)_{t_m+N_s+1}\}, \quad (2)$$

where $N_s = T_s/T$ is the number of data points in each data pack with T, T_s being the data and algorithm sampling times, respectively. This partitioning is convenient for online applications, as D^{t-1} should have been previously collected so that the algorithm can be executed from t_m to $t_m + N_s + 1$, an interval which we will define as algorithm time step t . Ultimately, inferences are completed at $t_m + N_s + 2$. Fig. 1 illustrates the timeline for the data and the algorithm. It is worth mentioning that the computation can be done simultaneously with the task in the adjacent algorithm step (e.g. phase A of algorithm t , phase B of algorithm $t-1$ and phase C of algorithm $t-2$ can all be done simultaneously).

According to Bayes' rule and assuming data points are independent and identically distributed (i.i.d) in Eq. (1), we have

$$P(\theta^t | [D^{t-1}, D^t]) = \frac{P(D^t | \theta^t, D^{t-1}) P(\theta^t | D^{t-1})}{\int P(D^t | \tau^t, D^{t-1}) P(\tau^t | D^{t-1}) d\tau^t}, \quad (3)$$

where θ^t denotes the parameters at current algorithm time steps. $P(\theta^t | D^{t-1})$ is the prior distribution over parameters, which is also the posterior distribution at the previous algorithm time step. Probability $P(D^t | \theta^t, D^{t-1})$ is the likelihood function which is obtained by sampling from the one-step-ahead prediction:

$$\hat{Y}^{t|t-1} = F(D^{t-1}, \theta^t), \quad (4)$$

where $\hat{Y}^{t|t-1}$ is a sample from the prediction of the output in (1). If the model in (4) is accurate, then the difference between the real output and predicted is the measurement noise, (i.e., $Y^{t|t-1} - \hat{Y}^{t|t-1} = \nu$). Therefore, the model

parameter may be updated as follows:

$$P(D^t|\theta^t, D^{t-1}) = \prod_{t=t_m+1}^{t_m+N_s+1} P_\nu(Y^{t|t-1} - \hat{Y}^{t|t-1}), \quad (5)$$

where P_ν is the probability distribution of noise. Note that there is no restriction on the type of noise probability distribution. A good approximation can be a Gaussian distribution with sample means and variances of the data as its parameters. For more information, please refer to the supplementary material.

Markov Chain Monte Carlo (MCMC)

MCMC is often employed to compute the posterior pdf numerically. The multidimensional integral in (3) is approximated by samples drawn from the posterior pdf. The samples are first drawn from a different distribution called proposal distribution, denoted $q(\cdot)$, which can be sampled more easily compared to the posterior. Brooks et al. (2011) discusses different types of MCMC implementations which may employ various proposal distributions and corresponding acceptance criteria. The main steps of the Metropolis-Hastings algorithm are listed as follows (Ninness and Henriksen 2010):

1. Set initial guess θ_0 while $P(\theta_0|Y) > 0$ for $k = 1$,
2. Draw candidate parameter θ_{cnd} , at iteration k , from the proposal distribution, $q(\theta_{cnd}|\theta_{k-1})$
3. Compute the acceptance probability,

$$\alpha(\theta_{cnd}|\theta_{k-1}) = \min \left\{ 1, \frac{P(\theta_{cnd}|D)q(\theta_{k-1}|\theta_{cnd})}{P(\theta_{k-1}|D)q(\theta_{cnd}|\theta_{k-1})} \right\}, \quad (6)$$

4. Generate a uniform random number γ in $[0, 1]$,
5. “Accept” candidate if $\gamma \leq \alpha$ and “ignore” it if $\gamma > \alpha$,
6. Set iteration to $k + 1$ and go to step 2.

Precision and reliability

Two important notions in probabilistic frameworks to compare results are precision (ϵ) and reliability (δ). The former represents the proximity of a sample to the ground truth, and the latter represents the probability that an accepted sample lies within ϵ of the ground truth.

Lemma: Let P_k to be the probability of k samples from MCMC, and $\mathbb{E}(P_k)$ to denote their expected value. According to Chernoff bound, to achieve the required precision and reliability $\epsilon, \delta \in [0, 1]$, as $Pr\{[P_k - \mathbb{E}(P_k)] \leq \epsilon\} \geq \delta$, the minimum number of samples (k) must satisfy the following relation (Tempo, Calafiore, and Dabbene 2012)

$$k \geq \frac{1}{2\epsilon^2} \log\left(\frac{2}{1-\delta}\right). \quad (7)$$

ARMCMC algorithm

At each algorithm time interval, ARMCMC recursively estimates the posterior pdf by drawing samples. The number of samples drawn is constrained by the desired precision and reliability, and the real-time requirement. On the other hand,

Algorithm 1: ARMCMC

Assumptions: 1) roughly noise mean (μ_ν) 2) roughly noise variance (σ_ν) 3) desired precision and reliability (ϵ_0, δ_0) 4) desired threshold for model mismatch (ζ_{th})

Goal: Online calculation of parameters posterior distribution given the consecutive t -th pack of data ($P(\theta^t|D^t)$)

Initialization: Prior knowledge for θ_1^0 , $n = 0$

Consider desired precision and reliability (ϵ, δ)

repeat

Put $t_0 = n * N_s + 1$ from (2), $n + +$

Add new data pack to dataset D^t

Model mismatch index: ζ^t from (10)

if $\zeta^t < \zeta_{th}$ **then**

Reinforcement: set prior knowledge equal to the latest posterior of previous pack

Temporal forgetting factor: λ^t from (9)

else

Modification: set prior knowledge θ_1^n

Temporal forgetting factor: $\lambda^t = 0$

end if

Set minimum iteration k_{min} from (12)

for $k = 1$ **to** k_{min} **do**

Proposal distribution:

• draw $\lambda_k \sim U(0, 1)$

• *Variable jump distribution:* $q_k^t(\cdot)$ from (8)

Draw $\theta_k^{t*} \sim q_k^t(\cdot)$

Acceptance rate: $\alpha(\cdot)$ from (6)

Draw $\gamma \sim U(0, 1)$

if $\gamma \leq \alpha$ **then**

‘Accept’ the proposal

end if

end for

Wait to build $D_{t_0}^{t_m+N_s+1}$ (algorithm sample time)

until No data is obtained

the maximum number of data points in each data pack (N_s) is limited by the frequency of model variation, and the minimum is confined by the shortest required time, such that the algorithm is real-time.

We propose a variable jump distribution that enables both exploiting and exploring. This will necessitate the definition of the temporal forgetting factor as a model mismatch measure to reflect current underlying dynamics of the data. We also prove that ARMCMC achieves the same precision and reliability with fewer samples compared to the traditional MCMC. Algorithm 1 summarizes ARMCMC.

Variable jump distribution

We propose a variable jump distribution (also known as a proposal distribution) to achieve faster convergence, thereby enabling real-time parameter estimation:

$$q_k^t(\theta^t|\theta_{k-1}^t) = \begin{cases} P(\theta^{t-1}|D^{t-1}) & \lambda_k \leq \lambda^t \\ N(\mu_D, \sigma_\nu) & \lambda_k > \lambda^t \end{cases}, \quad (8)$$

where θ_{k-1}^t is the $(k-1)$ -th parameter sample which is given by the t -th data pack throughout the MCMC evaluation. In each algorithm time sample, the averages of the second half

of this quantity will construct θ^t . $P(\theta^{t-1}|D^{t-1})$ is the posterior pdf of the parameters at the previous algorithm time step, and $N(\mu_D, \sigma_\nu)$ is a Gaussian distribution with its mean and variance μ_D, σ_ν computed using the empirical mean and variance of D^{t-1} if available.

Remark 1: Note that according to (Bishop 2006), ARMCMC is still a valid MCMC scheme since the variable jump policy does not violate the independency between samples. The reason is that the decision to whether select the proposal from previous samples or not is purely stochastic. The only difference is proposing more reasonable candidates with an adaptive threshold of acceptance. Further elaboration will be presented in following sections.

The hyperparameter λ^t is called *temporal forgetting factor* which is an adaptive threshold for the t -th pack that takes inspiration from classical system identification. This will regulate how previous knowledge affects the posterior pdf. Intuitively, a smaller value for λ^t means that there might be a larger/sudden change in the ground truth value, and thus more exploration is needed. Conversely, a larger value of λ^t is appropriate when θ is changing slowly, and therefore previous knowledge should be exploited. Exploiting this knowledge will lead to an overall better precision and reliability.

Temporal forgetting factor

Depending on the changes in the distribution of the parameter θ , a new sample can be drawn according to the *modification* or the *reinforcement* mode. Modification is employed to re-identify the distribution ‘from scratch’ while reinforcement is employed to make the identified probability distribution more precise when it is not undergoing sudden change. Therefore, we define a *model mismatch index*, denoted ζ^t , such that when it surpasses a predefined threshold ($\zeta^t > \zeta_{th}$), modification is applied. Otherwise ζ^t is used to determine λ^t as follows:

$$\lambda^t = e^{-|\mu_\nu - \zeta^t|}, \quad (9)$$

where μ_ν is an estimation of the noise mean, b the calculation of the expected value in Eq. (1). Note that employing modification is equivalent to setting $\lambda^t = 0$. The model mismatch index ζ^t itself is calculated by averaging the errors of the previous model given the current data:

$$\zeta^t = 1/N_s \sum_{n=1}^{N_s} \left(y_n^t - \mathbb{E}_{\theta \in \theta^{t-1}} (F(D^t(n), \theta)) \right), \zeta^0 = \infty \quad (10)$$

Remark 2: The model mismatch index accounts for all sources of uncertainty in the system. To calculate ζ_{th} , one needs to precalculate the persisting errors between the predicted and measured data. In other words, ζ_{th} is an upper bound for the unmodeled dynamics, disturbances, noises, and any other sources of uncertainty in the system.

Remark 3: To avoid numerical issues, the summation of probability logarithms are calculated. In addition, each data pair in the algorithm time sample is weighted based on its temporal distance to the current time. Therefore Eq. (5) is

modified as:

$$\log(P(\cdot)) = \sum_{t_m+1}^{t_m+N_s+1} \log P_\nu(e^t), \quad (11)$$

$$e^t = \left(Y_n^t - F^t(D^{t-1}(n), \theta^t) \right) e^{-\rho(N_s-n)},$$

where $\rho \in [0, 1]$ is a design parameter that reflects the volatility of the model parameters, and $e^t = [e_1^t, \dots, e_n^t, \dots, e_{N_s}^t]$. For systems with fast-paced parameters, ρ should take larger values.

Minimum required evaluation

Theorem 1. *Let ϵ and δ be the desired precision and reliability. Furthermore, assume that the initial sample has an enough number of evaluations. To satisfy the inequality in Eq. (7), the minimum number of samples k in ARMCMC is calculated using this implicit relation:*

$$k_{min} = \frac{1}{2\epsilon^2} \log\left(\frac{2}{\lambda^t(1-\delta) + 2(1-\lambda^t)e^{-2\epsilon^2(1-\lambda^t)k_{min}}}\right). \quad (12)$$

Proof. Samples from previous pdf: According to the variable jump distribution in (8), given k samples, the expected number of samples drawn from the previous posterior pdf ($P(\theta|D^t)$) is $\lambda^t k$. By assumption, the algorithm has already drawn at least k samples in the previous algorithm time-step. Consequently, by (7), the expected number of samples with distances less than ϵ from $\mathbb{E}(P_k)$ are drawn from a previous distribution of at least $\lambda k \delta$.

Samples from Gaussian: By (8), there are $k_0 = (1 - \lambda^t)k$ samples drawn in expectation. Based on this assumption, we have $Pr\left\{\{P_k - \mathbb{E}(P_k)\} \leq \epsilon\right\} \geq \delta_0$, where δ_0 is given by rearranging (7):

$$\delta_0 = 1 - 2e^{-2\epsilon^2 k_0}. \quad (13)$$

Thus, the expected number of samples with distances less than ϵ from $\mathbb{E}(P_k)$ are at least $\delta_0(1 - \lambda^t)k$.

Overall reliability: The total expected number of samples with distances less than ϵ from $\mathbb{E}(P_k)$ are the summation of the two parts mentioned above. Hence, it is obtained through dividing by k :

$$\delta_1 = \frac{(\lambda^t k \delta) + (\delta_0(1 - \lambda^t)k)}{k} \quad (14)$$

With the new obtained reliability, which is greater than the desired one, we can safely decrease the number of evaluations. For the sake of illustration, Fig. 2 presents the minimum required number of evaluations with respect to λ for different precisions and reliabilities. As it can be seen, the MCMC is equal to ARMCM if λ is always set to one. The number of evaluations in ARMCMC mitigates as the validity of the previous model increases. \square

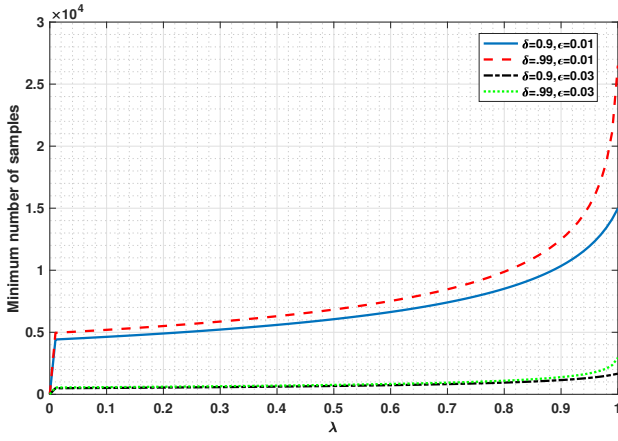


Figure 2: K_{min} with respect to λ for some values of ϵ, δ in ARMCMC. (for $\lambda = 1$ evaluation for ARMCMC is equivalent to MCMC)

Results

In this section, we demonstrate the performance of the proposed approach with two examples. First, we employ ARMCMC to identify parameters in the soft bending actuator model and compare the results by RLS and PF. In the second example, we evaluate our method on the Hunt-Crossley model when given a reality-based simulation, and compare it with a simple MCMC and RLS. All the results/code are available on <https://github.com/anonym-paper/ARMCMC/tree/submitted>.

Fluid soft bending actuator

Consider the dynamic model of a fluid soft bending actuator, given by (Wang et al. 2019):

$$\begin{aligned}\ddot{\alpha} &= q_1(p - p_{atm}) - q_2\dot{\alpha} - q_3\alpha, \\ u_c \text{sign}(p_s - p)\sqrt{|p_s - p|} &= q_4\dot{p} + q_5\ddot{p}, u_d = 0, \\ u_d \text{sign}(p - p_{atm})\sqrt{|p - p_{atm}|} &= q_6\dot{p} + q_7\ddot{p}, u_c = 0,\end{aligned}\quad (15)$$

where α is the angle of the actuator and u_c, u_d are the control inputs for retraction and contraction. Also, p, p_s, p_{atm} are the current, compressor and atmosphere pressure respectively. For this example, we assume $q_1 = 1408.50, q_2 = 132.28, q_3 = 3319.40$ are known and $p_{atm} = 101.3$ kPa, $p_s = 800$ kPa. We are trying to identify the remaining four parameters (q_4, \dots, q_7). To this end, we assume the hybrid model below:

$$u \text{sign}(\Delta p)\sqrt{|\Delta p|} = \theta_1\dot{p} + \theta_2\ddot{p}, u = \{u_c, u_d\}, \quad (16)$$

where Δp is either $(p_s - p)$ for retraction or $(p - p_{atm})$ for contraction, and θ_1 represents q_4, q_6 , while θ_2 represents q_5, q_7 . For RLS, as the range of parameters are small, we scale the input vector by a factor of 10^7 . Given the input (u_c, u_d) and the output (p, \dot{p}) , we want to identify the parameter and estimate the current angle of the actuator, assuming its initial position is at the origin.

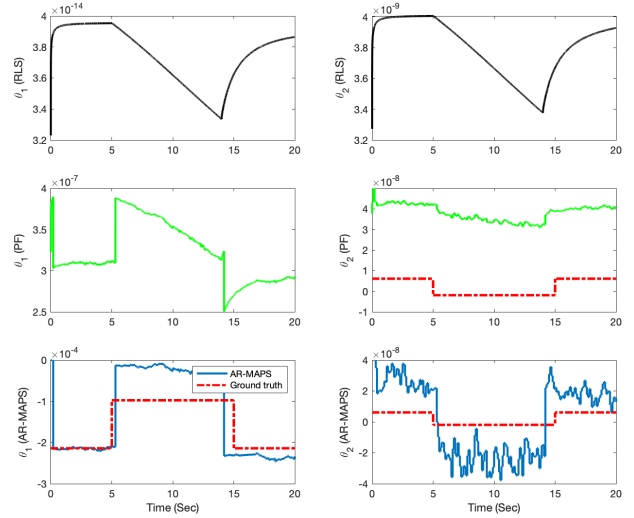


Figure 3: Parameter variation for RLS, AR-MAPS, and PF

Modeling for PF First, we derive the first order differential relation as follows:

$$\begin{aligned}\dot{x}_2 &= q_1(x_3 - p_{atm}) - q_2x_2 - q_3x_1 \\ \dot{x}_3 &= \frac{u \text{sign}(\Delta p)\sqrt{\Delta p}}{x_4 + x_5x_3}\end{aligned}\quad (17)$$

where the state space is $X = [x_1, \dots, x_5]^T = [\alpha, \dot{\alpha}, p, \theta_1, \theta_2]^T$ and $\dot{x}_1 = x_2, \dot{x}_4 = 0, \dot{x}_5 = 0$ which is a random walk. Eq. (17) is a nonlinear and hybrid model due to the relation of x_3 and the noise is reflected in the measurement sensor ($y = [p, \dot{p}, u_c, u_d]^T + \nu$). For PF, we need the state transition matrix which is the discretized version of (17), however, due to complexity, we need to further simplify the computation. For more information, please refer to supplementary material.

Quantitative analysis The data sample time is $T = 1$ ms and each data pack includes 100 samples which results in an algorithm sample time equal to $T_s = 100$ ms. The running time of the RLS approach is approximately 2 ms, however, for PF and ARMCMC it is limited by 10 ms, and 80 ms, respectively. Point estimation is obtained by considering the mode at the modification phase and the median during the reinforcement phase; this estimate is denoted as AR-MAPS. The true parameters with the means and standard deviations of the posterior probability using AR-MAPS are shown in Table 1. The parameter point estimate results are shown in Fig. 3. The estimation errors for θ_1, θ_2 , and prediction of angles ($\Delta\theta_1, \Delta\theta_2, \Delta\alpha$) for three recursive approaches are illustrated in Table 2. As seen, RLS provides an effective tracking error for θ_2 and requires less running time, however, the estimation error for θ_1 is relatively lower in AR-MAPS which will result in a superior final angle prediction. The estimation of the angle is plotted in Fig. 4.

Hunt-Crossley model

In this section, we demonstrate ARMCMC by identifying parameters of the Hunt-Crossley model, which represent

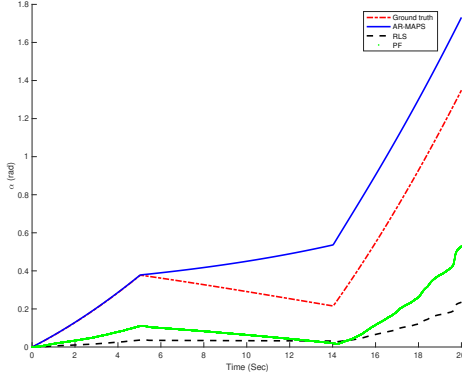


Figure 4: Angle of the actuator comparison of RLS and AR-MAPS for soft bending actuator.

Table 1: Summery of parameter estimation for AR-MAPS

PARAMETER	q_4	q_5	q_6	q_7
SCALE	10^{-4}	10^{-9}	10^{-5}	10^{-9}
TRUE	-2.14	6.12	-9.76	-1.90
POSTERIOR MEAN	-1.89	1.14	-11.43	-0.73
POSTERIOR S.D.	0.0041	0.21	0.0034	0.31

Table 2: Comparison of RLS, PF, and AR-MAPS for fluid soft bending actuator

METRIC	RLS	PF	AR-MAPS
$\ \Delta\theta_1\ $	0.0235	0.0233	0.0089
$\ \Delta\theta_2\ \times 10^{-6}$	0.60053	4.8517	2.6951
$\ \Delta\alpha\ $	61.4862	50.6386	32.4846
RUNNING TIME	2MS	10MS	80MS

an environment involving a needle contacting soft material. The needle is mounted as an end-effector on a high-precision robotic arm, which switches between two modes: free motion and contact. For medical applications, effectively mounting force sensors on the needle is typically infeasible due to sterilizing issues. Due to abrupt changes in the model parameters when the contact is established or lost, online estimation of the force is extremely challenging.

Contact dynamic model Consider the dynamics of contact as described by the Hunt-Crossley model, which is more consistent with the physics of contact than classical linear models such as Kelvin-Voigt (Haddadi and Hashtrudi-Zaad 2012). In order to overcome the shortcomings of linear models, (Hunt and Crossley 1975) proposed the following hybrid nonlinear model:

$$f_e(x(t)) = \begin{cases} K_e x^p(t) + B_e x^p(t) \dot{x}(t) & x(t) \geq 0 \\ 0 & x(t) < 0 \end{cases} \quad (18)$$

in which $K_e, B_e x^p$ denote the nonlinear elastic and viscous force coefficients, respectively. The parameter p is typically

between 1 and 2, depending on the material and the geometric properties of contact. Also, $x(t), \dot{x}(t), f_e$ are the current position, velocity (as input X), and contact force (as output Y) in Eq. (1). If $x \geq 0$, then the needle is inside the soft material. K_e, B_e, p are three unknown parameters (θ in Eq. (1)) that need to be estimated. For more information on the experimental data of the soft contact, please refer to the supplementary material. To relax the nonlinearity in the parameters, we use log:

$$\begin{aligned} \log(f_e) &= \log(K_e x_s^p + B_e \dot{x}_s x_s^p), \\ \log(f_e) &= p \log(x_s) + \log(K_e + B_e \dot{x}_s). \end{aligned} \quad (19)$$

For RLS, we also need to further simplify the relation by assuming $B_e/K_e \dot{x}_s \ll 1$. Note that the vector of parameters (θ) are not independent, which may lead to divergence.

$$\begin{aligned} \log(1 + B_e/K_e \dot{x}_s) &\approx B_e/K_e \dot{x}_s, \\ \log(f_e) &= p \log(x_s) + \log(K_e) + B_e/K_e \dot{x}_s. \end{aligned} \quad (20)$$

$$\begin{aligned} U &= [1, \dot{x}_s, \log(x_s)], \\ \theta &= [\log(K_e), B_e/K_e, p]^T. \end{aligned} \quad (21)$$

Setup The data structure is the same as the previous simulation. Prior distribution of all three parameters (K_e, B_e, p) are initialized to $N(1, 0.1)$ (a normal distribution with $\mu = 1$ and $\sigma = 0.1$) as a non-informative initial guess, whereas after applying the control effort and availability of the first data pack, these distributions are updated. Moreover, as more data is collected, the spread of the posterior pdf decreases. After around 5 seconds, the needle goes outside of the soft material, and has zero force; this is equivalent to all parameters being set to zero. The color-based visualization of the probability distribution over time is used for the three parameters in Fig. 5. During the period of time that the entire space is blue (zero probability density), there is no contact and the parameter values are equal to zero.

Since we are taking a Bayesian approach, we are able to estimate the entire posterior pdf. However, for the sake of illustration, the point estimates are computed from the ARMCMC algorithm by using AR-MAPS method. The results are shown in Fig. 6 for the time-varying parameters $\theta_1 = K_e, \theta_2 = B_e, \theta_3 = p$. During the times that RLS results are chattering due to the use of saturation (if not, the results would have diverged), the needle is transitioning from being inside the soft material to the outside or vice versa. In addition, due to the assumption (20), performance can decrease even when there is no mode transition. Although in the RLS approach estimated parameters suddenly diverged during free motion as the regression vectors are linearly dependent, with ARMCMC this is not an issue. The result of force prediction is presented in Fig. 7, which shows the effect of two different identification approaches. This probability of interest can be easily obtained by deriving the parameter density at one's disposal. As we can see, The RLS, and MCMC suffer from numerous high frequency responses due to the level of uncertainty and identification error.

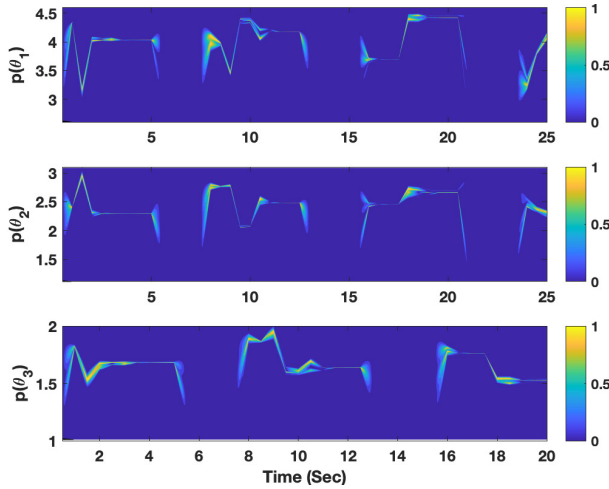


Figure 5: Probability distribution of parameters ($\theta_1 = K_e, \theta_2 = B_e, \theta_3 = p$) using ARMCMC.

Quantitative comparison Quantitative details of comparing a naive point estimate of the ARMCMC algorithm by averaging the samples (denoted as AR-APS) and the RLS method are listed in Table 3. This reveals an improvement of over 70% in the precision of all model parameters throughout the study by using the Mean Absolute Error (MAE) criteria. The force estimation error also had more than 55% improvement. Among parameters, the viscose (B_e) has the largest error in the RLS method since it is underestimated due to the restrictive assumption in Eq. (20). The AR-MAPS approach uplifts the performance of the parameter identification and the force estimation. The ARMCMC algorithm paves the way for successful online identification of model parameters while restrictive presumptions are neglectable. Meanwhile, by employing the strength in the Bayesian paradigm, this powerful tool can cooperate different sources of knowledge. The recursion in the Bayesian optimization framework provides a suboptimal solution for the identification of nonlinear, hybrid, non-Gaussian systems. We also compare ARMCMC to MCMC. For real-time implementation, MCMC requires more time to converge. In this example, with $\lambda = 0.7$, the value of k_{min} is 15000 for MCMC but only 6000 for ARMCMC with $\epsilon = 0.01, \delta = 0.9$. Two possible ways to address this drawback in MCMC are to reduce the number of samples to 5000 per algorithm iteration (denoted MCMC-1 in Table 3), which results in worse precision and reliability compared to ARMCMC, or to increase the algorithm sample time to 0.2 (denoted MCMC-2 in Table 3) which would cause more delay in the estimation result and slower responses to changes in the parameter.

Conclusions

This paper presented an adaptive recursive MCMC algorithm for online identification of model parameters with full probability distribution. When applied to systems involving abrupt changes of model parameters, conventional approaches suffer from low performance. Results on the Hunt-Crossley and fluid soft bending actuator as nonlinear hy-

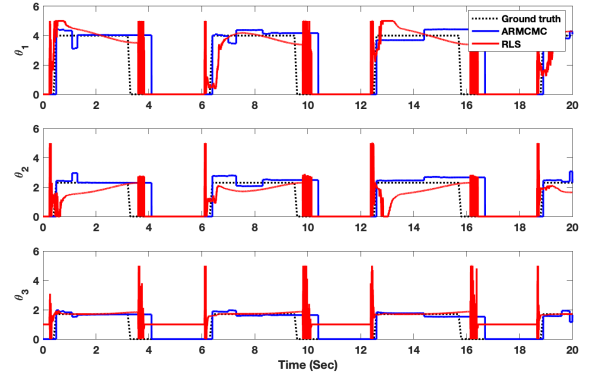


Figure 6: Model parameters ($\theta_1 = K_e, \theta_2 = B_e, \theta_3 = p$) point estimation in AR-MAPS.

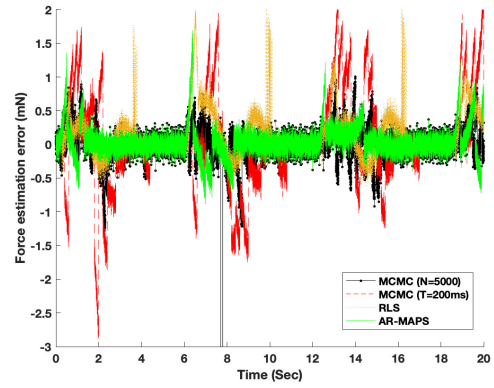


Figure 7: Force prediction error profile.

Table 3: Comparison of RLS and point estimate of ARMCMC and MCMC for environment identification.

ERRORS (MAE)	K_e	B_e	p	F_e (MN)
RLS	0.5793	0.9642	0.3124	51.745
MCMC-1	0.6846	0.8392	0.3783	76.695
MCMC-2	0.7294	0.9964	0.4195	101.88
AR-APS	0.0774	0.0347	0.0945	33.774
AR-MAPS	0.0617	0.0316	0.0756	31.659

brid dynamic models was compared with well-known conventional identification approaches. The proposed method adapted quickly to abrupt changes and relaxes the prerequisite conditions in the parameters. Since ARMCMC is a more general approach, it can be applied to a wider range of systems. In the case of single-mode nonlinear systems with LIP condition, one may use RLS which provides the best result 40x faster compared to ARMCMC. However, for hybrid/multi-modal systems with fairly accurate parametric models, ARMCMC can output reasonable online inferences. They can be fairly accurate since the uncertainty in the models can be captured in the probability distribution of the parameters. However, this option is not available for conventional approaches like RLS or KF. For PF as another

sampling-based methods for online Bayesian optimization, it relies on the dynamical model of evolution to enhance the acceptance of the proposal distribution. Nonetheless, in the case of parameter identification, as the evolution model for parameters is a random walk, there is no extra knowledge for the estimator. PF as a sequential Monte Carlo (SMC) method assumes a connectivity in updating parameters in the resampling phase, therefore, ARMCMC surpasses PF performance in parameter identification problems.

References

- Agand, P.; and Shoorehdeli, M. A. 2019. Adaptive Model Learning of Neural Networks with UUB Stability for Robot Dynamic Estimation. In *2019 International Joint Conference on Neural Networks (IJCNN)*, 1–6. IEEE.
- Agand, P.; Taghirad, H. D.; and Khaki-Sedigh, A. 2016. Particle filters for non-gaussian Hunt-Crossley model of environment in bilateral teleoperation. In *4th International Conference on Robotics and Mechatronics (ICROM)*, 512–517. IEEE.
- Agand, P.; Taherahmadi, M.; Lim, A.; and Chen, M. 2022. Human Navigational Intent Inference with Probabilistic and Optimal Approaches. In *2022 International Conference on Robotics and Automation (ICRA)*, 8562–8568. IEEE.
- Bishop, C. M. 2006. Pattern recognition. *Machine Learning*, 128.
- Brooks, S.; Gelman, A.; Jones, G.; and Meng, X.-L. 2011. *Handbook of markov chain monte carlo*. CRC press.
- Carvalho, A. S.; and Martins, J. M. 2019. Exact restitution and generalizations for the Hunt–Crossley contact model. *Mechanism and Machine Theory*, 139: 174–194.
- Green, P. J. 1995. Reversible jump Markov chain Monte Carlo computation and Bayesian model determination. *Biometrika*, 82(4): 711–732.
- Green, P. L. 2015. Bayesian system identification of a nonlinear dynamical system using a novel variant of simulated annealing. *Mechanical Systems and Signal Processing*, 52: 133–146.
- Haddadi, A.; and Hashtrudi-Zaad, K. 2012. Real-time identification of Hunt-Crossley dynamic models of contact environments. *IEEE transactions on robotics*, 28(3): 555–566.
- Hoffman, M. D.; Gelman, A.; et al. 2014. The No-U-Turn sampler: adaptively setting path lengths in Hamiltonian Monte Carlo. *J. Mach. Learn. Res.*, 15(1): 1593–1623.
- Houssein, E. H.; Helmy, B. E.-d.; Rezk, H.; and Nassef, A. M. 2021. An enhanced Archimedes optimization algorithm based on Local escaping operator and Orthogonal learning for PEM fuel cell parameter identification. *Engineering Applications of Artificial Intelligence*, 103: 104309.
- Hunt, K.; and Crossley, F. 1975. Coefficient of restitution interpreted as damping in vibroimpact. *Journal of applied mechanics*, 42(2): 440–445.
- Joho, D.; Tipaldi, G. D.; Engelhard, N.; Stachniss, C.; and Burgard, W. 2013. Nonparametric Bayesian models for unsupervised scene analysis and reconstruction. *Robotics: Science and Systems VIII*, 161.
- Khatibisepehr, S.; Huang, B.; and Khare, S. 2013. Design of inferential sensors in the process industry: A review of Bayesian methods. *Journal of Process Control*, 23(10): 1575–1596.
- Kim, S. H.; Nam, E.; Ha, T. I.; Hwang, S.-H.; Lee, J. H.; Park, S.-H.; and Min, B.-K. 2019. Robotic machining: A review of recent progress. *International Journal of Precision Engineering and Manufacturing*, 20(9): 1629–1642.
- Kuśmierczyk, T.; Sakaya, J.; and Klami, A. 2019. Variational Bayesian Decision-making for Continuous Utilities. In Wallach, H.; Larochelle, H.; Beygelzimer, A.; d Alché-Buc, F.; Fox, E.; and Garnett, R., eds., *Advances in Neural Information Processing Systems 32*, 6392–6402. Curran Associates, Inc.
- Lin, C.-S. 2019. Frequency-domain approach for the parametric identification of structures with modal interference. *Journal of Mechanical Science and Technology*, 33(9): 4081–4091.
- Mandel, T.; Liu, Y.-E.; Brunskill, E.; and Popovic, Z. 2016. Efficient Bayesian Clustering for Reinforcement Learning. In *IJCAI*, 1830–1838.
- Ninness, B.; and Henriksen, S. 2010. Bayesian system identification via Markov chain Monte Carlo techniques. *Automatica*, 46(1): 40–51.
- Nori, A.; Hur, C.-K.; Rajamani, S.; and Samuel, S. 2014. R2: An efficient MCMC sampler for probabilistic programs. In *Proceedings of the AAAI Conference on Artificial Intelligence*, volume 28.
- Saar, K. A.; Giardina, F.; and Iida, F. 2018. Model-free design optimization of a hopping robot and its comparison with a human designer. *IEEE Robotics and Automation Letters*, 3(2): 1245–1251.
- Tempo, R.; Calafiore, G.; and Dabbene, F. 2012. *Randomized algorithms for analysis and control of uncertain systems: with applications*. Springer Science & Business Media.
- Tobar, F. 2018. Bayesian Nonparametric Spectral Estimation. In Bengio, S.; Wallach, H.; Larochelle, H.; Grauman, K.; Cesa-Bianchi, N.; and Garnett, R., eds., *Advances in Neural Information Processing Systems 31*, 10127–10137. Curran Associates, Inc.
- Wang, B.; Sekhon, A.; and Qi, Y. 2018. A Fast and Scalable Joint Estimator for Integrating Additional Knowledge in Learning Multiple Related Sparse Gaussian Graphical Models. In Dy, J.; and Krause, A., eds., *Proceedings of the 35th International Conference on Machine Learning*, volume 80 of *Proceedings of Machine Learning Research*, 5161–5170. Stockholmsmässan, Stockholm Sweden: PMLR.
- Wang, T.; Zhang, Y.; Chen, Z.; and Zhu, S. 2019. Parameter identification and model-based nonlinear robust control of fluidic soft bending actuators. *IEEE/ASME Transactions on Mechatronics*, 24(3): 1346–1355.
- Welling, M.; and Teh, Y. W. 2011. Bayesian learning via stochastic gradient Langevin dynamics. In *Proceedings of the 28th international conference on machine learning (ICML-11)*, 681–688. Citeseer.

Williams, G.; Goldfain, B.; Drews, P.; Saigol, K.; Rehg, J.; and Theodorou, E. A. 2018. Robust sampling based model predictive control with sparse objective information. In *Robotics Science and Systems*.

Yang, B.; Wang, J.; Zhang, X.; Yu, T.; Yao, W.; Shu, H.; Zeng, F.; and Sun, L. 2020. Comprehensive overview of meta-heuristic algorithm applications on PV cell parameter identification. *Energy Conversion and Management*, 208: 112595.

Yu, H.; Li, J.; Ji, Y.; and Pecht, M. 2022. Life-cycle parameter identification method of an electrochemical model for lithium-ion battery pack. *Journal of Energy Storage*, 47: 103591.